Oxide minerals in the Liqhobong kimberlite, Lesotho

NABIL Z. BOCTOR AND F. R. BOYD

Geophysical Laboratory, Carnegie Institution of Washington
Washington, D. C. 20008

Abstract

The oxide minerals in kimberlite from Liqhobong, Lesotho, are represented by discrete ilmenite nodules, groundmass ilmenite, spinel solid solutions, and perovskite. The discrete ilmenite nodules have margins that are enriched in Mg (15–21 weight percent MgO) relative to the cores (11–13 weight percent MgO). The Mg enrichment is restricted to the outermost margins of the nodules (300–500 μm) and is believed to be of metasomatic origin. The groundmass ilmenite has a Mg content similar to that of the margins of the discrete ilmenite nodules but is more enriched in Fe_2O_3. Spinels are represented by two distinct varieties: a titanian–ferrian pleonaste that belongs to the Mg_2TiO_4–Fe_2TiO_4–$FeAl_2O_4$–$MgAl_2O_4$ solid solution series and trends in composition toward $MgFe_2O_4$ and Fe_3O_4, and a titanian aluminous chromite that belongs to the $FeCr_2O_4$–$MgCr_2O_4$–$FeAl_2O_4$–$MgAl_2O_4$ solid solution series. The titanian aluminous chromite apparently crystallized as a liquidus phase prior to the crystallization of titanian pleonaste from the late-stage Ti-rich fluids that reacted with the ilmenite nodules. The perovskite is Nb-bearing and is rich in rare-earth elements (4.8–6.1 weight percent REE oxides). It is enriched in light REE relative to heavy REE. The enrichment of perovskite in REE may be related to partitioning of these elements between perovskite and an immiscible carbonate liquid or to equilibration of perovskite with a CO_2-rich fluid enriched in light REE.

Introduction

The physical and chemical changes undergone by kimberlite magma during its eruption and crystallization remain puzzling problems. Valuable insights can be gained by study of groundmass minerals in kimberlite and of late-stage reactions between kimberlitic minerals and the residual fluids of kimberlite magma. Boyd and Clement (1977) described metasomatic zoning in olivine from the De Beers kimberlite, and Haggerty *et al.* (1979) reported two types of zoning in ilmenite nodules from Monastery kimberlite, a "magmatic zoning trend" toward enrichment in $MgTiO_3$ and a "kimberlite reaction trend" toward enrichment in $FeTiO_3$ and $MnTiO_3$. Haggerty (1973) and Boctor and Meyer (1979) also described complex reaction mantles on ilmenite nodules in kimberlite and discussed their significance as indicators of the redox conditions prevailing during the reaction between the nodules and late-stage kimberlitic fluids.

A petrographic and electron microprobe study of ilmenite nodules and associated oxide minerals in the groundmass in the Liqhobong kimberlite was undertaken in order to extend the present understanding of late-stage reactions during the crystallization of kimberlitic magma.

Geological setting and petrography

The Liqhobong intrusion comprises a large circular main pipe (330 m in diameter) and a small satellite pipe (95 m in diameter) joined to the main pipe by a dike (Nixon and Boyd, 1973). The dike consists of anastomosing kimberlite stringers that merge to a width of 1–2 m and expand to the southeast into a "blow." The southeast blow is about 20 m across and is conspicuous for its masses of dark bluish-gray "hardebank" with abundant olivine and subordinate ilmenite in a groundmass containing calcite, serpentine, perovskite, and phlogopite. Nixon and Boyd (1973) described two varieties of olivine in the hardebank from the southeast blow: large, rounded crystals and small, euhedral crystals that overlap in composition in the range Fo = 86–95. The rounded olivine crystals are similar in their trace-element chemistry to olivines from the granular ultramafic nodules in the hardebank but include more ferriferous varieties. The euhedral crystals, however, are

believed to have crystallized from the kimberlitic magma and are richer in trace elements than the rounded ones. In the present study ten samples from the southeast blow were investigated.

Methods of study

The specimens were studied in both reflected and transmitted light. Electron microprobe analyses were performed with an automated MAC-500 electron microprobe. For data reduction of ilmenite and spinel analyses, the correction schemes of Bence and Albee (1968) and Albee and Ray (1970) were used. The MAGIC IV computer program of Colby (1971) was used for data reduction of the perovskite analyses. The program corrects for interferences between characteristic X-ray spectra of the rare-earth elements (REE) and other elements, in addition to the standard corrections for deadtime, background atomic number, absorption, and fluorescence factors. Although the accuracy of the microprobe analyses of the REE present in trace amounts is much lower than that of neutron activation analyses, electron microprobe analysis seems to be the only feasible technique for determination of REE in perovskite from kimberlite because of the difficulty of separating pure concentrations of this mineral for analysis by other methods. It is also possible to study grain-to-grain variation within individual specimens by using the electron microprobe.

Oxide mineralogy and chemistry

The oxide minerals in the hardebank from the southeast blow of the Liqhobong kimberlite are represented by (a) discrete ilmenite nodules displaying complex reaction mantles, (b) perovskite in the groundmass and in reaction mantles on ilmenite nodules, and (c) groundmass spinels that occasionally are associated with groundmass ilmenite.

Ilmenite

Ilmenite is present mainly as discrete nodules ranging in size from a few millimeters up to 1.5 cm. The nodules occur as large single crystals showing uniform extinction when observed under crossed nicols or as interlocking polycrystalline aggregates showing different optic orientations. Each nodule is surrounded by reaction mantles of spinel, secondary ilmenite, and perovskite. These reaction mantles were described in detail by Haggerty (1973) and will not be discussed here. Electron microprobe analyses of several ilmenite nodules (Table 1) show that they are rich in Mg and Cr. The MgO content of ilmenite

ranges between 10.5 and 21 weight percent. The high MgO concentrations are characteristic of the outermost zones adjacent to the reaction mantles in each nodule. Detailed electron microprobe traverses across several of the nodules (see Fig. 1, for example) confirmed this observation. Magnesium enrichment is restricted to a distance between 300 and 500 μm from the margins. Beyond this narrow zone of Mg enrichment, the MgO content of the nodules is much lower and is almost constant. Similar Mg enrichment was observed by Haggerty (1973) in an ilmenite nodule from a single specimen of Liqhobong kimberlite. Our investigation indicates that such enrichment is characteristic of ilmenite nodules in Liqhobong kimberlite. Within individual nodules, no enrichment of Cr, unlike Mg, was observed in the margins. When the MgO content of all the ilmenite nodules is plotted against the Cr_2O_3 content, a tendency for increase in Cr content with increase in Mg content is observed in the cores of nodules but not in the rims (Fig. 2).

When the microprobe analyses are recalculated in terms of the molecular proportions of $MgTiO_3$, $FeTiO_3$, and Fe_2O_3, the $MgTiO_3$ of the nodules is 38.1–65.7 mole percent, the $FeTiO_3$ content is 27.6–56.1 mole percent, and the Fe_2O_3 content is 5.2–9.2 mole percent (Fig. 3). For the cores of the nodules, however, the range is much narrower, 38.1–45.8 mole percent for $MgTiO_3$, 48–56 mole percent for $FeTiO_3$, and 5.2–8.0 mole percent for Fe_2O_3.

A few idiomorphic ilmenite crystals (15–30 μm) are present in the groundmass. Their MgO content is in the range 15.1–17.3 weight percent, comparable to MgO concentrations in the rims of ilmenite nodules, and their Cr_2O_3 content is 2.55–3.47 weight percent. Their Fe_2O_3 content, however, is higher (9.4–10.8 mole percent) in comparison to that of the nodules.

Groundmass spinels

Groundmass spinels are rare in the Liqhobong pipe. Two distinct types of spinels were recognized microscopically and by electron microprobe analyses (Table 2, Fig. 4)—an Al-bearing titanian chromite and a titanian–ferrian pleonaste. The two types of spinels occur in rocks that are petrographically similar, but do not coexist in the same specimen. The titanian chromite occurs as euhedral crystals, which appear to be homogeneous in composition and do not show zoning or reaction mantles. The titanian–ferrian pleonaste occurs mostly as subhedral to euhedral crystals that are more common in the groundmass in the vicinity of the reaction mantles on ilmenite nodules. It is more enriched in Fe_2O_3 rela-

Table 1. Representative electron microprobe analyses of ilmenite

	2003b Nodule		2003b	175		176	
	Rim	Core	Groundmass ilmenite	Rim	Core	Rim	Core
SiO$_2$	< 0.01	< 0.01	< 0.01	< 0.01	< 0.01	< 0.01	< 0.01
TiO$_2$	55.95	52.32	52.12	53.66	52.58	53.09	52.64
Al$_2$O$_3$	0.26	0.30	0.34	0.45	0.40	0.60	0.65
Cr$_2$O$_3$	1.64	1.54	2.55	2.41	2.36	2.98	3.00
Fe$_2$O$_3$	7.85	7.27	11.24	7.76	6.70	7.48	6.91
FeO	14.68	26.62	15.91	16.96	24.98	19.97	23.75
MnO	0.70	0.68	0.66	0.80	0.55	0.65	0.50
MgO	19.59	11.07	16.99	17.10	12.20	15.17	12.92
CaO	< 0.01	< 0.01	< 0.01	< 0.01	< 0.01	< 0.01	0.04
Total	100.67	99.81	99.81	99.13	99.76	99.99	100.40

tive to the pleonaste in the reaction mantles. Fe$_2$O$_3$/FeO ranges between 1.431 and 1.929 for the groundmass pleonaste *vs.* 1.345 for pleonaste in the reaction mantles. No zoning was observed in titanian–ferrian pleonaste. When the chemical analyses of the spinels in the Liqhobong pipe are plotted in the spinel prism (Fig. 4), the two varieties of spinel plot as two separate populations showing markedly different Cr/(Cr + Al) and Ti/(Ti + Cr + Al). The analyses of the Al-bearing titanian chromite plot on the base of the spinel prism, whereas the analyses of the titanian–ferrian pleonaste plot on its front rectangular face.

Perovskite

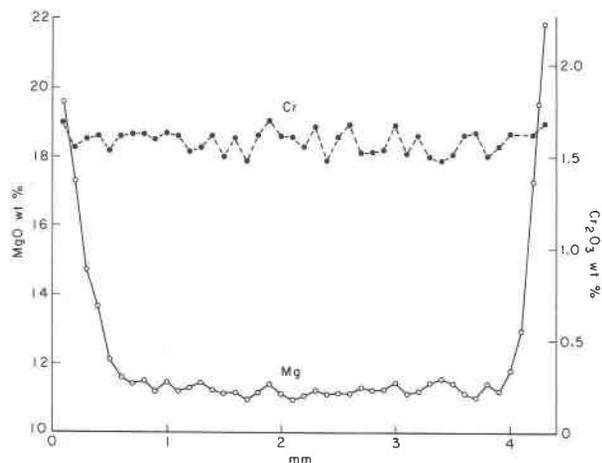All the rocks studied contain more perovskite than groundmass spinels and ilmenite. The perovskite is Nb-bearing and is rich in REE (Table 3). It displays little variation in composition from one sample to another. The Nb$_2$O$_5$ content ranges from 0.48 to 0.93 weight percent. Apparently Nb substitutes for Ti and the electrostatic charge is balanced by simultaneous substitution of Na and REE for Ca. The sum of the REE oxides ranges between 4.84 and 6.08 percent. Perovskite seems to be more enriched in the light rare-earth elements (LREE) relative to the heavy rare-earth elements (HREE). The most abundant REE is Ce (2.20–2.54 weight percent Ce$_2$O$_3$), followed by Nd (0.88–1.53 weight percent Nd$_2$O$_3$) and La (0.25 to 0.71 weight percent La$_2$O$_3$).

Discussion

A comparison of the data on the composition of ilmenite in the Liqhobong kimberlite with analyses reported by Boyd and Nixon (1973), Mitchell (1973, 1977), and Pasteris *et al.* (1979) for other kimberlites
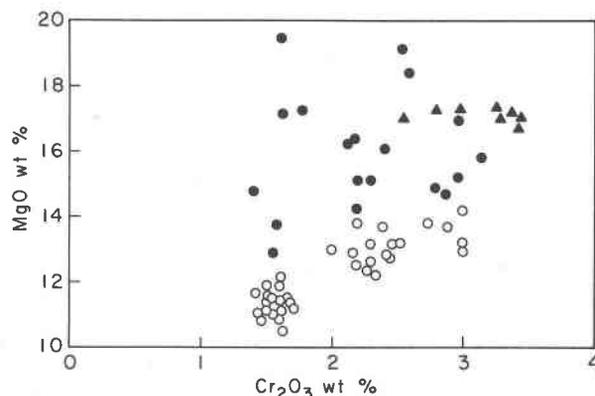

Fig. 1. Microprobe traverse across a discrete ilmenite nodule showing the changes in MgO and Cr$_2$O$_3$ content from core to rim.

Fig. 2. MgO *vs.* Cr$_2$O$_3$ content of discrete ilmenite nodule cores (open circles) and rims (solid circles), and groundmass ilmenite (solid triangles).
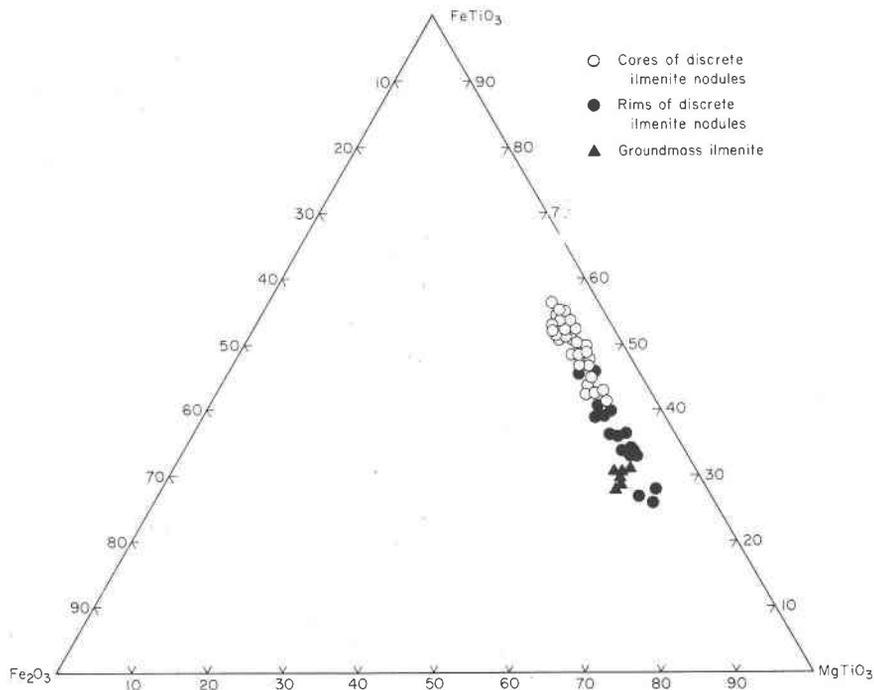
Fig. 3. Composition of discrete ilmenite nodules and groundmass ilmenites in terms of their $MgTiO_3$, $FeTiO_3$, and Fe_2O_3 content.

supports their suggestion that the Mg content of il-menite from different kimberlites may vary widely. For example, the Liqhobong ilmenite is richer in Mg than the ilmenite from Monastery, Kao, and Arturo de Paiva kimberlites and overlaps in composition with those from Premier and Frank Smith. The Mg contents of ilmenites from Kao and Liqhobong kim-berlites are quite different, although these pipes are only 5 km apart.

Zoning in discrete ilmenite nodules in kimberlite seems to be more common than was previously be-lieved. Haggerty *et al.* (1979) described two zoning trends in ilmenite nodules from Monastery, a "mag-matic zoning trend" toward enrichment of $MgTiO_3$ from core to margin and a "kimberlite reaction trend" toward enrichment in $FeTiO_3$ and MnO and depletion in $MgTiO_3$. Haggerty *et al.* attributed the magmatic trend to reaction with a liquid caused by a

Table 2. Representative electron microprobe analyses of spinels*

	2003b				173			
	1	2	3	4	1	2	3	4
SiO_2	0.46	0.70	0.13	0.28	0.18	0.25	0.18	0.33
TiO_2	20.07	19.54	23.29	19.47	5.74	5.79	6.25	7.71
Al_2O_3	12.37	12.30	9.72	12.53	12.96	13.06	11.53	14.41
Cr_2O_3	1.17	1.04	2.09	0.97	38.74	37.51	37.52	30.44
Fe_2O_3	26.23	26.79	23.71	26.96	10.27	10.31	10.92	14.26
FeO	15.84	15.73	16.58	14.48	17.22	16.67	17.18	14.99
MnO	0.96	1.03	1.09	1.04	0.68	0.70	0.69	0.75
MgO	23.18	23.04	24.03	23.20	13.91	14.06	13.70	16.57
CaO	0.10	0.14	0.11	0.16	0.09	0.11	0.14	0.25
Total	100.38	100.30	100.69	99.09	99.79	98.46	98.16	99.71

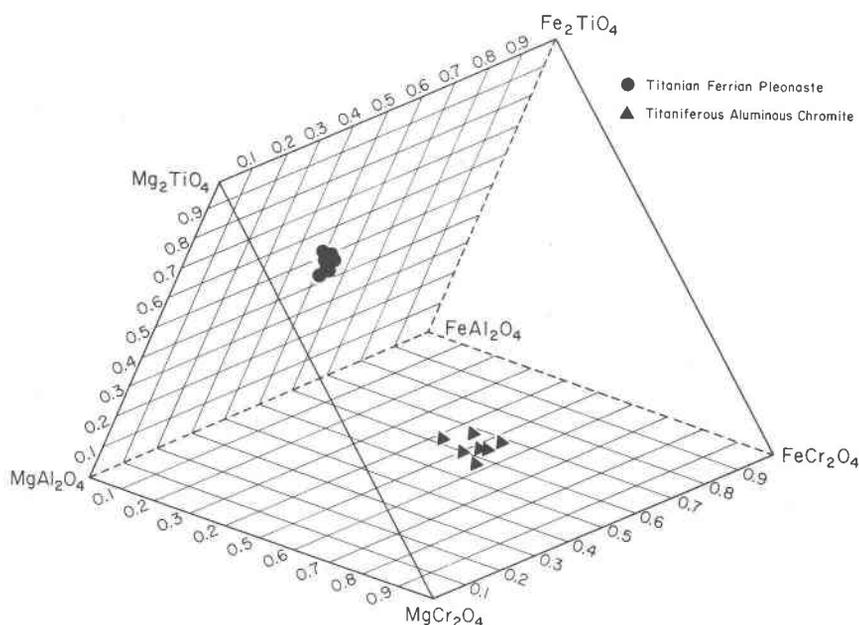*All analyses are of groundmass spinels.

Fig. 4. Groundmass spinel analyses plotted in the spinel prism.

decrease in the total pressure. A consequence of this trend was a decrease in f_{O_2} manifested by the observed decrease in Fe_2O_3 toward the nodule margins at Monastery. The kimberlite reaction trend was considered by Haggerty *et al.* to be late-stage and related to carbonatite liquid immiscibility, and it may have taken place during the incorporation of the nodules in the kimberlite.

The zoning observed in ilmenite nodules from Liqhobong kimberlite differs from the magmatic zoning described by Haggerty *et al.* in ilmenite nodules from Monastery. There is no progressive increase in $MgTiO_3$ from core to rim in Liqhobong ilmenite nodules, and there is no decrease in Fe_2O_3 content toward the margins of the nodules as at Monastery. The zoning in the ilmenite nodules in Liqhobong kimberlite seems to be metasomatic in origin and is believed to have originated through nodule interaction with Mg-rich fluids. The limited extent of the zone of Mg enrichment relative to nodule size, the fact that the Mg content across the major part of the nodules is nearly constant, the occurrence of Mg-rich spinels in the reaction mantles surrounding the ilmenite nodules, and the similarity in Mg content between the nodule rims and groundmass ilmenite seem to support this interpretation.

The metasomatic zoning in the ilmenite nodules from Liqhobong kimberlite and the kimberlite reaction trend observed in Monastery ilmenite nodules are both products of late-stage reactions, but

the reaction paths in the two cases are different. At Liqhobong the reaction trend was toward enrichment of Mg, which is the reverse of the kimberlite reaction trend at Monastery. A clue to the cause of these two different reaction paths can be found by comparing the compositions of the phases in the reaction mantles on the ilmenite nodules in both kimberlites. At Liqhobong the Mg-rich margins of the nodules are mantled by magnesioferrite ulvöspinel and titanian–ferrian pleonaste (Haggerty, 1973) rich in Mg and Ti but with a low to moderate Fe_2O_3 content. At Monastery the Mg-depleted margins of the ilmenite nodules are mantled by strongly zoned titanian magnetite and Ti-poor magnetite. Thus, the factors that apparently controlled the two different reaction paths observed in the Liqhobong and Monastery ilmenite nodules are $Mg/(Mg + Fe^{2+})$ in the fluid and the oxygen fugacity. The metasomatic zoning in the ilmenite nodules at Liqhobong was induced by a fluid with a higher $Mg/(Mg + Fe^{2+})$ and a lower f_{O_2} than that which caused the zoning in the Monastery ilmenite nodules.

Metasomatic zoning in kimberlitic olivine was reported by Boyd and Clement (1977) in the peripheral kimberlite at De Beers. The zoning is mainly restricted to the outer 100–150 μm and includes both reverse and normal varieties, but regardless of the trend the zoning tends to converge on a rim composi-

Table 3. Representative electron microprobe analyses of perovskite

	1	2	3	4	5	6
SiO_2	0.04	0.00	0.00	0.28	0.08	0.02
TiO_2	54.28	54.67	54.63	54.62	54.38	54.52
FeO	1.24	1.09	1.29	1.30	1.12	1.18
MgO	0.34	0.21	0.39	0.34	0.38	0.31
CaO	36.54	36.93	35.59	36.11	36.50	36.51
Na_2O	0.79	0.73	0.64	0.70	0.63	0.71
Y_2O_3	0.00	0.00	0.00	0.28	0.00	0.13
La_2O_3	0.67	0.52	0.58	0.78	0.66	0.65
Ce_2O_3	2.41	2.37	2.66	2.45	2.29	2.38
Pr_2O_3	0.05	0.00	0.11	0.00	0.02	0.00
Nd_2O_3	1.14	0.88	0.91	0.95	1.31	1.07
Sm_2O_3	0.03	0.39	0.13	0.27	0.33	0.25
Eu_2O_3	0.08	0.32	0.00	0.00	0.33	0.15
Gd_2O_3	0.29	0.37	0.26	0.41	0.33	0.35
Tb_2O_3	0.04	0.08	0.00	0.00	0.00	0.00
Dy_2O_3	0.00	0.18	0.04	0.00	0.00	0.00
Ho_2O_3	0.00	0.00	0.00	0.02	0.00	0.00
Er_2O_3	0.05	0.01	0.05	0.00	0.00	0.00
Tm_2O_3	0.00	0.00	0.00	0.00	0.00	0.00
Yb_2O_3	0.16	0.09	0.00	0.00	0.08	0.01
Lu_2O_3	0.09	0.00	0.05	0.19	0.00	0.00
Nb_2O_5	0.79	0.71	0.93	0.60	0.87	0.74
Total	99.02	99.66	98.27	99.01	99.29	98.98
Atomic proportions on the basis of 3 oxygens						
Si	0.00	0.00	0.00	0.00	0.00	0.00
Ti	0.965	0.965	0.977	0.933	0.965	0.969
Fe	0.023	0.020	0.027	0.027	0.023	0.023
Mg	0.012	0.008	0.016	0.012	0.012	0.012
Ca	0.926	0.930	0.906	0.914	0.920	0.926
Na	0.035	0.035	0.031	0.031	0.027	0.031
Y	0.00	0.00	0.00	0.004	0.00	0.00
La	0.008	0.004	0.004	0.008	0.004	0.004
Ce	0.020	0.020	0.023	0.020	0.020	0.020
Pr	0.00	0.00	0.00	0.00	0.00	0.00
Nd	0.008	0.008	0.008	0.008	0.012	0.008
Sm	0.00	0.004	0.00	0.004	0.004	0.004
Eu	0.00	0.004	0.00	0.004	0.004	0.00
Gd	0.004	0.004	0.004	0.00	0.004	0.004
Tb	0.00	0.00	0.00	0.00	0.00	0.00
Dy	0.00	0.00	0.00	0.00	0.00	0.00
Ho	0.00	0.00	0.00	0.00	0.00	0.00
Er	0.00	0.00	0.00	0.00	0.00	0.00
Tm	0.00	0.00	0.00	0.00	0.00	0.00
Yb	0.00	0.00	0.00	0.00	0.00	0.00
Lu	0.00	0.00	0.00	0.00	0.00	0.00
Nb	0.008	0.008	0.012	0.008	0.008	0.008
Total	2.008	2.008	2.008	2.012	2.008	2.008

tion of Fo 89–90. Crystals with cores more Mg-rich than this range have predominantly normal zoning, whereas those with cores more Fe-rich than this range have predominantly reverse zoning.

The olivine crystals in Liqhobong kimberlite have serpentinized margins, and any zoning patterns they might have displayed are now destroyed. The serpentinization of olivine precluded correlation between ilmenite and olivine zoning in the Liqhobong kimberlite. Note, however, that the metasomatic zoning observed by Boyd and Clement (1977), like that observed in ilmenite nodules, is also primarily controlled by the $Mg/(Mg + Fe^{2+})$ of the fluid and the oxygen fugacity. The $Mg/(Mg + Fe^{2+})$ probably was not constant during late-stage reactions; however, in a general way, olivine with $Mg/(Mg + Fe^{2+})$ higher than that of the fluid reacted to form more iron-rich rims, whereas olivine with $Mg/(Mg + Fe^{2+})$ lower than that of the fluid reacted to form more Mg-rich rims. The convergence of the two zoning trends to a narrow compositional range at the margins was apparently controlled by the $Mg/(Mg + Fe^{2+})$ of the fluid and the fO_2 prevailing in the final stages of the reaction.

The two populations of groundmass spinels observed in Liqhobong kimberlite now appear to be characteristic of many kimberlites. The spinels closest in composition to the titanian pleonaste from Liqhobong kimberlite are those from Benfontein (Dawson and Hawthorne, 1973; Boctor and Boyd, 1979) and the groundmass spinels from Green Mountain kimberlite (Boctor and Meyer, 1979, Table 1). The Ti-rich spinels in the Peuyuk and Tunraq kimberlites were considered by Mitchell and Clark (1976) and Mitchell (1979) as members of the magnesian ulvöspinel–ulvöspinel–magnetite solid solution series. These spinels, however, contain 6 to 8 weight percent Al_2O_3, which suggests that they contain pleonaste in solid solution but are more enriched in total Fe and Fe_2O_3 relative to those from Liqhobong, Benfontein, and Green Mountain kimberlites, which belong to the quaternary system Mg_2TiO_4–Fe_2TiO_4–$FeAl_2O_4$–$MgAl_2O_4$ and show trends toward $MgFe_2O_4$ and Fe_3O_4. The titanian aluminous chromite is similar in composition to that described by Mitchell and Clark (1976) and is essentially a member of the quaternary system $FeCr_2O_4$–$MgCr_2O_4$–$FeAl_2O_4$–$MgAl_2O_4$. The titanian aluminous chromite possibly crystallized as a liquidus phase prior to the crystallization of titanian pleonaste from the late-stage Ti-rich fluids that reacted with the ilmenite nodules.

The similarity in composition of the titanian pleonaste in the reaction mantles on ilmenite nodules and in the groundmass supports this suggestion.

The perovskite in the Liqhobong kimberlite shows a Nb content comparable to that given by Mitchell (1972) for kimberlitic perovskite. It also shows the same pattern of enrichment in LREE observed in perovskite from Yakutian kimberlite (Blagulkina and Tarnovskaya, 1975) and from Green Mountain kimberlite (Boctor and Meyer, 1979). Kimberlite from Yakutia, however, has a lower total REE content (total REE < 2.0 weight percent) and that from Green Mountain has a higher REE content (total REE oxides 5.9 to 10.31 weight percent) relative to that from Liqhobong. The REE content of the Liqhobong perovskite, however, is higher than that previously reported for kimberlites from southern Africa (Grantham and Allen, 1960). No data are available on the distribution of REE in whole-rock kimberlite from Liqhobong to compare the perovskite REE pattern with the whole-rock pattern.

Rare-earth elements are known to form complexes with various volatiles, such as CO_2 (Kosterin, 1959; Ganeyev, 1962; Balashov and Krigman, 1975), F (Bandurkin, 1961; Mineyev, 1963; Mineyev et al., 1966), and Cl (Flynn and Burnham, 1978). In the Liqhobong kimberlite, perovskite occurs in close association with calcite in the groundmass and as reaction rims on the spinels that mantle the ilmenite nodules. These observations suggest that perovskite started to crystallize after the separation of an immiscible carbonate liquid from the kimberlite magma and apparently continued to crystallize from the late-stage fluids that reacted with the ilmenite nodules. These fluids are known to be enriched in CO_2 and H_2O. Wendlandt and Harrison (1979) showed that partitioning of REE between coexisting silicate and carbonate melts favors the carbonate melts, especially for HREE. When a CO_2 vapor is present, however, the LREE are fractionated preferentially into the vapor relative to the carbonate melt. Wendlandt and Harrison also found that the enrichment of REE in CO_2 vapor is approximately 3 to 4 orders of magnitude greater than that in water vapor at 5 kbar and of the same order of magnitude as that in water vapor at 20 kbar. It is not known, however, whether the pattern observed for REE in perovskite was caused by partitioning of these elements between perovskite and the carbonate melt or whether it was caused by equilibration of perovskite with a residual CO_2-rich fluid enriched in LREE. An experimental investiga-

tion of the partitioning of REE between perovskite, carbonate melt, and CO_2 vapor is needed to clarify this problem.

Acknowledgments

References

Albee, A. L. and L. Ray (1970) Correction factors for electron probe microanalysis of silicates, oxides, carbonates, phosphates, and sulfates. *Anal. Chem., 42,* 1408–1414.

Balashov, A. Y. and L. D. Krigman (1975) The effect of alkalinity and volatiles on rare earth separation in magmatic systems. *Geochem. Int., 12,* 165–170.

Bandurkin, G. A. (1961) Behavior of the rare earths in fluorine-bearing media. *Geochemistry (USSR),* No. 2, 159–167.

Bence, A. E. and A. L. Albee (1968) Empirical correction factors for the electron microanalysis of silicates and oxides. *J. Geol., 76,* 382–403.

Blagulkina, V. H. and A. N. Tarnovskaya (1975) Perovskite from Yakutian kimberlite (in Russian). *Zap. Vses. Mineral. Obshch., 104,* 703–710.

Boctor, N. Z. and F. R. Boyd (1979) Oxide minerals in layered kimberlite–carbonate sills from Benfontein, South Africa. *Carnegie Inst. Wash. Year Book, 78,* 493–496.

—— and H. O. A. Meyer (1979) Oxide and sulfide minerals in kimberlite from Green Mountain, Colorado. In F. R. Boyd and H. O. A. Meyer, Eds., *Kimberlites, Diatremes, and Diamonds (Proc. 2d Int. Kimberlite Conf.,* Vol. 1, p. 217–228). American Geophysical Union, Washington, D. C.

Boyd, F. R. and C. R. Clement (1977) Compositional zoning of olivine in kimberlites from the De Beers Mine, Kimberley, South Africa. *Carnegie Inst. Wash. Year Book, 76,* 485–493.

—— and P. H. Nixon (1973) Origin of the ilmenite–silicate nodules in kimberlites from Lesotho and South Africa. In P. H. Nixon, Ed., *Lesotho Kimberlites,* p. 254–268. Lesotho National Development Corporation, Maseru, Lesotho.

Colby, J. W. (1971) *MAGIC IV, a computer program for quantitative electron microprobe analysis.* Bell Telephone Laboratories, Allentown, Pennsylvania.

Dawson, J. B. and J. B. Hawthorne (1973) Magmatic sedimentation and carbonatitic differentiation in kimberlite sills at Benfontein, South Africa. *J. Geol. Soc. London, 129,* 61–85.

Flynn, R. T. and C. W. Burnham (1978) An experimental determination of rare earth partition coefficients between a chloride containing vapor phase and silicate melts. *Geochim. Cosmochim. Acta, 42,* 685–701.

Ganeyev, I. G. (1962) On the possible transport of matter in the form of complicated complex compounds. *Geochemistry (USSR),* No. 10, 1042–1049.

Grantham, D. R. and J. B. Allen (1960) Kimberlites in Sierra Leone. *Overseas Geol. Miner. Resour., 8,* 5–25.

Haggerty, S. E. (1973) Spinels of unique composition associated with ilmenite reaction mantles in the liqhobong kimberlite pipe, Lesotho. In P. H. Nixon, Ed., *Lesotho Kimberlites,* p. 149–158. Lesotho National Development Corporation, Maseru, Lesotho.

——, R. B. Hardie III and B. M. McMahon (1979) The mineral chemistry of ilmenite nodules associations from the Monastery diatreme. In F. R. Boyd and H. O. A. Meyer, Eds., *The Mantle Sample (Proc. 2d Int. Kimberlite Conf.,* Vol. 2, p. 249–256). American Geophysical Union, Washington, D.C.

Kosterin, A. V. (1959) The possible modes of transport for the rare earths by hydrothermal solutions. *Geochemistry (USSR),* No. 4, 381–387.

Mineyev, D. A. (1963) Geochemical differentiation of the rare earths. *Geochemistry (USSR),* No. 12, 1129–1149.

——, D. P. Yu, B. P. Sobovev and V. L. Borutskaya (1966) Differentiation of rare earth elements under supercritical conditions. *Geochem. Int., 3,* 357–359.

Mitchell, R. H. (1972) Composition of perovskite in kimberlite. *Am. Mineral., 57,* 1748–1753.

—— (1973) Magnesian ilmenite and its role in kimberlite petrogenesis. *J. Geol., 81,* 301–311.

—— (1977) Geochemistry of magnesian ilmenites from kimberlites from South Africa and Lesotho. *Lithos, 10,* 29–37.

—— (1979) Mineralogy of the Tunraq kimberlite, Somerset Island, N.W.T., Canada. In F. R. Boyd and H. O. A. Meyer, Eds., *Kimberlites, Diatremes, and Diamonds (Proc. 2d Int. Kimberlite Conf.,* Vol. 1, p. 161–169). American Geophysical Union, Washington, D.C.

—— and D. B. Clark (1976) Oxide and sulfide mineralogy of the Peuyuk kimberlite, Somerset Island, N.W.T., Canada. *Contrib. Mineral, Petrol., 56,* 157–172.

Nixon, P. H. and F. R. Boyd (1973) The Liqhobong intrusion and kimberlitic olivine composition. In P. H. Nixon, Ed., *Lesotho Kimberlites,* p. 141–148. Lesotho National Development Corporation, Maseru, Leotho.

Pasteris, J. D., F. R. Boyd and P. H. Nixon (1979) The ilmenite association at the Frank Smith Mine, R.S.A. In F. R. Boyd and H. O. A. Meyer, Eds., *The Mantle Sample (Proc. 2d Int. Kimberlite Conf.,* Vol. 2, p. 265–278). American Geophysical Union, Washington, D.C.

Wendlandt, R. F. and W. J. Harrison (1979) Rare earth element partitioning between coexisting immiscible carbonate and silicate liquids and CO_2 in the system $K_2O–Al_2O_3–SiO_2–CO_2$ and implications for the formation of light rare earth element enriched rocks. *Contrib. Mineral. Petrol., 69,* 409–419.